

Internal Stress, Lattice Deformation, and Modulus of Polymers

ANQIU ZHANG,* HAO JIANG,** ZONGQUAN WU, CHENXUN WU, and BAOJUN QIAN

Man-made Fiber Research Institute, China Textile University, Shanghai, People's Republic of China

SYNOPSIS

The relationships among internal stress, lattice deformation, and the moduli of polymers, such as poly(ethylene terephthalate) (PET), polypropylene (PP), polyethylene (PE), polyacrylonitrile (PAN), and poly(*p*-phenylene terephthalamide) (PPTA), have been studied systematically. Compared to small molecule crystals, polymer crystals have many more defects and their parameters of the crystal unit cells and the density of the crystalline region are easy to vary to a certain extent. During the processing, external stresses were put on the polymer fibers and polymer molecules were drastically deformed, which induced polymer crystallization and preferred orientation. After processing, there are many macromolecules frozen in the nonequilibrium status, which is the cause of internal stress. Heat treatment could give energy to the macromolecules to release the internal stress and to approach thermodynamic equilibrium. For polymer crystals, the higher the annealing temperature, the shorter the lengths of the unit cell axes, the more integral and regular the crystal lattice, and the smaller the unit cell volume. Crystalline modulus changes not only with different kinds of polymer materials, but also with measurement temperature and processing history. Polymer processing, mainly drawing, causes orientation and internal stress which causes lattice deformation and raises tensile modulus of polymer materials.

INTRODUCTION

Recently, there has been an increase in active study on the internal stresses of polymer fibers, although this research topic is not a novel one.¹⁻¹⁴ The reason is that along with the progress in technique and theory, scientists are not only able to get the precise data of the internal stress (see APPENDIX) but they are also able to begin to reveal its fundamental relationship between the structure and mechanical properties of polymers.¹⁵

In order to obtain outstanding properties for polymer fibers, the drawing and heat treatment should be carried out to make the macromolecules choose preferred orientation and to induce crystal-

lization if possible. The external force put on the fibers changes the macromolecular conformations greatly and drastically. Some molecules arrange along the fiber-axis direction and some stack into crystal lattices. After these procedures, perhaps there is a very small amount of the polymer molecules in the thermodynamic equilibrium status, however, most are frozen in the thermodynamically unstable position. There is always a tendency for molecules to go from the nonequilibrium to the thermodynamic equilibrium state, i.e., in order to reach the minimum energy status, the fiber molecules located in the crystal defect areas (which exist in greater numbers in polymers than in small molecule materials) would try to stack into complete and regular lattices; molecules in the amorphous areas would change their extended conformations toward coiled arrangements. In other words, there exists internal stresses frozen in polymer molecules which tend to change the macromolecules from thermodynamic nonequilibrium to equilibrium.

In principle, any method which has the capability of creating suitable situations to assist fiber mole-

* To whom correspondence should be sent; present address is Department of Polymer Science, University of Akron, Akron, OH 44325-3909.

** Present address: Department of Materials Science and Engineering, Georgia Institute of Technology, School of Textile & Fiber Engineering, Atlanta, GA 30332-0295.

Journal of Applied Polymer Science, Vol. 42, 1779-1791 (1991)
© 1991 John Wiley & Sons, Inc. CCC 0021-8995/91/061779-13\$04.00

cules into changing their nonequilibrium status toward equilibrium would liberate the "stored" internal stresses. The commonest and easiest way is by heating. By raising the temperature together with holding the fiber sample length constant, the internal stresses can be measured as the thermal shrinkage stresses. The heating contributes energy to the polymer molecules and helps them to overcome a series of intermediate barriers and releases the frozen internal stresses.¹¹ There are two kinds of thermal shrinkage stress measurements which are normally used. One is to elevate the temperature continuously with constant heating rate and to measure the corresponding shrinkage stress (method A, see APPENDIX); the other is to jump rapidly to a certain temperature and then measure the corresponding shrinkage stress (method B, APPENDIX). Because of the time and temperature dependencies of the thermal shrinkage stress, the latter method diminishes the relaxation effect of the fiber macromolecules; however, the information on the thermal movement at different molecular interaction levels is diminished as well. By the former method, the thermal movements of the molecules at various levels can be observed, but gradually increasing the temperature hurts the precision of the thermal shrinkage stress measurement. For glassy polymers, the thermal shrinkage stress reaches the maximum value then gradually reduces to zero at a certain elevated temperature. For most crystalline polymers, the thermal shrinkage stress also increases then reduces with increasing temperature, but at a certain temperature, it will remain at a particular plateau

level unless the temperature is higher than the melting point.¹⁰

In this paper, the lattice deformation and modulus variation for different polymer fibers are investigated through a systematic study of internal stresses. A universal relationship between the internal stress and modulus has been disclosed. It has also been proven that the internal stress is one of the main effects on the macroscopic tensile modulus of the polymer materials.

LATTICE DEFORMATION

The study of lattice deformation is a useful method to reveal the mechanism of variations in crystal modulus of polymers.¹⁶ The polymer crystallite is not as integral as the small molecule crystal and its structural regularity and size normally have wide distributions, hence, its x-ray diffraction spots are not as sharp either. It is difficult to precisely measure the angle (2θ) of the diffraction profile, which greatly influences the determination of the unit cell parameters. In order to take a convenient and accurate measurement, crystallographers usually anneal their samples under ultimate conditions (such as at the highest possible temperature, i.e., near melting point, without tension and with the longest time in order to make the crystallites integral and regular, to increase crystallinity and to make the profile function parameter of the crystalline peaks as unified as possible) (Table I). From the viewpoint of macromolecule entanglement, annealing with ex-

Table I Crystallinity, Crystal Size and Profile Function Parameter of PET Fiber

	Heat-Setting Condition					
	Unset	130° 15 min	160° 15 min	190° 15 min	220° 15 min	220° 4 h
Density (g/cm ³)	1.368	1.381	1.389	1.399	1.415	—
Crystallinity (%) (from density)	0.292	0.404	0.471	0.555	0.682	—
Crystallinity (%) (from WAXS)	0.63	0.74	0.78	0.80	0.85	0.86
Crystal size (Å):						
Crystal face (010)	16.82	19.30	24.16	50.36	75.90	99.69
Crystal face (100)	9.70	13.00	14.50	21.17	34.90	37.36
Crystal face (103)	11.79	17.60	24.64	35.04	44.52	76.06
Profile function parameters:						
Crystal face (010)	-0.100	0.001	0.000	0.010	0.200	0.300
Crystal face (100)	-0.800	0.010	0.010	0.100	0.550	0.600
Crystal face ($\bar{1}03$)	-0.500	0.040	0.180	0.300	0.600	0.620

tremely long times at high temperature could make crystal dislocations out of the crystallites and make crystalline regions more integral and increase the crystalline density.¹⁷ Namely, this kind of treatment makes the crystallinity, crystallite size and other crystalline parameters of polymers approach "optimization," eliminates the internal stresses, and results in sharp diffraction spots on the x-ray diffraction pattern and allows precise measurement of the crystal parameters. The melting points (MP) of so-annealed polymer crystals are close to the so-called equilibrium or thermodynamic melting points. Such kinds of polymer materials are brittle. Both their strength and modulus would drop drastically. Therefore, out of concern for commercial procedures

and practical applications, one needs to know not only the exact thermodynamic MP but also the apparent (or nonequilibrium) MP (or its range). For the same reason, one also needs to know the unit cell parameters both in equilibrium and deformed states, in which most of the commercial polymer products lie.

PET

Some polymers, e.g., cellulose, PE, PP, and PA, have more than one allomorphic crystal. However, PET is not allomorphic although the processing parameters, especially those of drawing and heat treatment

Table II PET Unit-Cell Parameters Published by Various Authors

Samples* and Authors	Density (g/cm ³)	<i>a</i> (Å)	<i>b</i> (Å)	<i>c</i> (Å)	α (deg.)	β (deg.)	γ (deg.)	<i>V</i> (Å ³)	Published Year
Fiber, heat-set at 230° for 8 h, by Astbury et al. ¹⁸	1.471	5.54	4.14	10.86	107°5'	112°24'	92°23'	216.8	1946
Fiber, drawn at 75°C, heat-set with constant length at 210°C, by Daubeny and Bunn ¹⁹	1.455	4.56	5.94	10.75	98.5°	118°	112°	219.2	1954
Kilian et al. ²⁰	1.495	d (100)	3.40			(Bunn 3.46)			1960
		d (010)	5.02			(Bunn 5.06)			
Film, uniaxially drawn to 700%, heat-set at 180°C, by Tomashpol'skii et al. ²¹	1.479	4.52	5.98	10.77	101.3°	118°	111°	215.6	1964
Fiber, heat-set at 250° with const. length, by Fakirov et al. ²²	1.515	4.48	5.85	10.75	99.5°	118.4°	111.2°	210.5	1975
Fiber treated at 100°	1.484								1975
Kinoshita et al. ²³	1.501	4.50	5.90	10.76	100.3°	118.6°	110.8°		1979
Zahn et al. ²⁴	1.501	d (010)	5.02			(Bunn 5.06)			1957
		d (100)	3.4			(Bunn 3.46)			
		d (010)	5.0			(Bunn 5.06)			
Lin et al. ²⁵	1.510								
Annealed Film		d (100)	3.45						1982
Fiber		d (010)	5.03						
		d (100)	3.40						
Film		d (010)	5.01						
Thistlethwaite et al. ²⁶	1.486	4.54	5.87	10.71	99.1	119.2	110.1	214.7	1988
annealed film with const. length, draw ratio: 5.4									
ratio: 6.0	1.501	4.53	5.87	10.73	99.6	119.6	110.6	212.5	1988

* The crystals of all these samples belong to the triclinic system.

Table III The Variations of Unit-cell Parameters of PET Fibers

	Heat-Setting Condition					
	Unset	130° 15 min	160° 15 min	190° 15 min	220° 15 min	220° 4 h
<i>a</i> (Å)	4.81	4.77	4.68	4.64	4.64	4.61
<i>b</i> (Å)	6.14	6.08	5.92	5.90	5.87	5.82
<i>c</i> (Å)	11.10	10.95	10.79	10.70	10.63	10.51
α (deg.)	99.2	97.6	95.1	94.2	93.9	93.8
β (deg.)	118.7	119.2	119.3	119.5	119.6	110.9
γ (deg.)	111.7	112.3	113.1	113.7	113.9	114.7
<i>V</i> (Å ³)	242.9	235.6	224.2	219.4	216.7	209.0
Density (g/cm ³)	1.31 ± 0.03	1.35 ± 0.03	1.42 ± 0.02	1.45 ± 0.01	1.47 ± 0.02	1.52 ± 0.03
Interplanar spacing deviation* (Å)	0.025	0.025	0.017	0.007	0.018	0.030
Internal stress:						
(MPa)	39.5	4.20	3.19	2.17	1.30	0.0668
(g/den)	0.345	0.0346	0.0262	0.0178	0.0107	0.000549

* Interplanar spacing deviation $\sum |\nabla|/n$, where $\nabla = d(\text{experiment}) - d(\text{calculation})$, and $n = \text{number of crystal plane}$.

(HT), can vary in a rather wide range, with processing even possible at low temperatures.

During the last 40 years, the reported PET unit cell parameters have shown a tendency that with ongoing time, the values of the unit cell volume decrease and the values of the unit cell density increase (Table II¹⁸⁻²⁶). Density of crystalline region (or unit cell) for PET has increased from 1.455 to 1.515 g/cm³. Owing to the progresses in instrument accuracy and computation, the experimental errors of recent data have obviously been reduced. Up to now, however, for the calculation of crystallinity the crystalline density has been chosen as 1.455, not 1.515. If the number 1.515 was adopted, the crystallinity calculated would be reduced by about 33%. Why do we still choose the *old* and *inaccurate* number, not the *new* and *accurate* one? The reason will be described as follows.

The unit cell parameters of high-speed-spinning PET fiber with relaxation at different temperatures are shown in Table III.¹⁷ The density of the crystalline region changes from 1.35 to 1.52 g/cm³. The change in crystal density is caused by the variation in crystal unit cell structure. It is clear that different annealing temperatures, tensions, and annealing times lead to different unit cell structures and crystal densities, which result in different internal stresses (Table III). The sample annealed at 190°C, similar to commercial PET fibers, has a unit cell density of 1.45. Hence, for normal PET fibers we should only choose the crystalline density to be 1.45 because the conventional HT makes the crystalline density approach 1.455, not 1.515.

Crystalline structures of a series of solid-state extruded PET samples have also been studied.²⁷ Their crystals are stress-induced. The experimental

Table IV Unit-Cell Parameters of Solid-State-Extruded PET

Extrusion Temperature	90°C						70°C		Annealed 220° 4 h
	10.0	6.0	3.5	6.0	5.0	3.5	—		
Extrusion ratio	10.0	6.0	3.5	6.0	5.0	3.5	—		
<i>a</i> (Å)	4.37	4.43	4.48	4.42	4.46	4.46	4.61		
<i>b</i> (Å)	5.87	5.93	5.98	5.93	5.89	6.06	5.82		
<i>c</i> (Å)	11.57	11.45	11.38	11.43	11.31	11.29	10.51		
α (deg.)	100.1	99.8	99.0	96.6	98.5	99.5	93.8		
β (deg.)	113.4	113.8	114.0	114.6	113.7	114.5	119.9		
γ (deg.)	111.4	113.8	114.0	112.7	112.0	111.9	114.7		
<i>V</i> (Å ³)	234.5	236.5	239.9	233.7	236.3	238.8	209.0		
Density (g/cm ³)	1.36 ± 0.02	1.35 ± 0.01	1.33 ± 0.01	1.37 ± 0.02	1.35 ± 0.01	1.34 ± 0.01	1.52 ± 0.03		

Table V PET Amorphous Structure

Solid State Extrusion at 50°C			
Extrusion ratio	6.0	5.0	3.5
Maximum distance between molecules (Å)	5.0	5.4	5.4
Minimum distance between molecules (Å)	3.4	3.2	3.2
Molecular distance distribution (Å)	1.6	2.2	2.3
Average molecular distance (Å)	4.0	4.0	4.0

results infer that in solid-state extruded PET there are many defects in the crystalline regions and the internal stress is comparatively high for this structure since the lattice deformation is large (up to 10%) (Table IV). At the same extrusion ratio, the change in the *c*-axis increases for high temperature extrusions.

In oriented amorphous PET produced by solid state extrusion at 50°C with three extrusion ratios, the average distance between PET molecules are all 4 Å, corresponding to a diffraction angle (2θ) of about 22° (Table V). The smallest distance we measured were from 3.2–3.4 Å, which is approximately equal to the (100) interplanar spacing 3.396 Å.²⁶ The benzene ring and most of the atoms in PET molecules lay on the (100) crystal plane. Thus, this distance reflects the average distance between benzene rings of neighboring PET molecules. It is also distinct that the minimum distance between benzene rings in oriented amorphous PET approaches the (100) interplanar spacing. The higher the extrusion rate, the narrower the range of molecular distances between the starting and end points of x-ray diffraction curves. Due to the variation of the starting and end point position of the diffraction diffraction, there does not exist a standard x-ray dif-

fraction curve of amorphous PET. In other words, the diffraction curve of amorphous PET is variable. The conformations and arrangements of the PET molecules in the amorphous area affect the internal stress.

PP and PE

Compared to PET, the differences of the unit cell parameters for PE- or PP-oriented fibers and isotropic bulks by different crystallographers are rather small (Table VI^{28–32} and VII^{33–38}). Obviously, this is caused by their low glass transition temperatures (PE: –120°C to –70°C; PP: –10°C). Therefore, even at room temperature, the annealing procedure can occur. The fluctuation of the PE or PP unit cell volume is also reduced owing to the improvement of polymer sample preparation techniques and instrumentation.

Tables VIII A and B and IX show the relationship between the *c*-axis length of the unit cell and internal stress (method A, APPENDIX).³⁹ It is unexpected for the internal stress to reduce with relaxation, and the variation of the PE unit cell could not evidently be observed. The reason why PE has different behavior from that of PP is that the internal stresses of both PE and PP are of the same order, but the lattice modulus of PE is one order higher than that of PP, 270, and 34 GPa, respectively. Hence the lattice deformation of PE could not be estimated easily by WAXD. The molecular weight and the number of entanglement joints should have an effect on the internal stress and the unit cell.

For gel-spun and ultra-drawn (draw ratio 40–50) PE fibers, because of their high molecular weights ($M_w = 1.57 \times 10^6$) and remaining molecular entanglements, our data show that PE have obvious lattice deformation, especially at the *a* and *b* axes (Table VIIIB).⁴⁰ The corresponding internal stress is over 10 MPa.

Table VI Unit-Cell Parameters of PE (Orthorhombic)

Crystal Density (g/cm ³)	<i>a</i> (Å)	<i>b</i> (Å)	<i>c</i> (Å)	<i>V</i> (Å ³)	Authors
1.008	7.40	4.93	2.534	92.45	Bunn (1939) ²⁸
1.011	7.36	4.94	2.534	92.13	Walter (1956) ²⁹
0.9988					Swan (1960) ³⁰
0.9998	7.406	4.936	2.547	93.16	Swan (1962) ³⁰
0.991					Kojima (1962) ³¹
0.9972	7.418	4.946	2.546	93.41	Zugenmaier (1969) ³²

Table VII Unit-Cell Parameters of PP (Monoclinic)

Crystal Density (g/cm ³)	<i>a</i> (Å)	<i>b</i> (Å)	<i>c</i> (Å)	(°)	<i>V</i> (Å ³)	Authors
0.931	6.69	6.504	20.98	99.5	900.4	Chiba (1964) ³³
0.938	6.65	6.50	20.96	99.3	894.1	Natta (1960) ³⁴
0.940	6.64	6.51	20.88	98.7	892.2	Mfncik (1960) ³⁵
0.946	6.66	6.495	20.78	99.62	886.2	Turner-Jones (1969) ³⁶
0.947	6.65	6.50	20.73	99.0	885.0	Hikosaka (1969) ³⁷
0.949	6.63	6.504	20.78	99.5	883.8	Wilchinsky (1960) ³⁸

PAN

Our annealing study on PAN fibers⁴¹ has indicated that during annealing there are displacements of the diffraction angles of the (100) and (110) interplanar spacings. But when the temperature returns to room temperature, the diffraction peaks also return to their original positions, i.e., the changes in 2θ are reversible in a certain heat-treatment temperature range. The extension of crystalline interplanar spacing during heating is consistent with the thermal expansion coefficient of PAN. PAN has a paracrystalline structure, and the diffraction spots on the meridian are smeared such that it is difficult to determine the variation of the *c*-axis. This reversibility might possibly be one of the characteristics of paracrystalline polymers.

PPTA

As a semirigid chain polymer crystal, the difference of the unit cell parameters of PPTA from different

Table VIIIA Unit-Cell Parameters and Internal Stress of PE

Annealing Condition	<i>a</i> (Å)	<i>b</i> (Å)	<i>c</i> (Å)	<i>V</i> (Å ³)	Internal Stress (MPa)
Unset	7.40	4.91	2.55	91.9	—
80°C					
15 min	7.41	4.91	2.53	92.1	—
90°C					
15 min	7.39	4.90	2.54	92.0	7.45
100°C					
15 min	7.40	4.90	2.54	92.1	6.37
110°C					
15 min	7.41	4.91	2.54	92.4	5.49
120°C					
15 min	7.39	4.91	2.54	92.2	5.10
Published data ²⁸	7.40	4.93	2.54	92.5	

authors is small (Table X⁴²⁻⁴⁵). The lattice modulus (157 GPa) is of the same order of PE.

The effects of tension and relaxed heat treatments on the *c*-axis of the PPTA unit cell is shown in Figure 1.⁴⁶ Extrapolating the linear relationship between the thermal shrinkage stress and the *c*-axis length⁴⁶ (at room temperature) to a thermal shrinkage stress of zero yields a *c*-axis length of 12.75 Å. From this value, we are able to calculate the strain (%) of the *c*-axis of the samples. The variation of strain, which is less than 2%, is consistent with that of thermal shrinkage stress. Perhaps, the high lattice modulus (as for PE) is the reason causing the low lattice strain.

INTERNAL STRESS AND MODULUS

Internal stress is caused by freeze drawing force during polymer fiber processing. It can be exhibited as a thermal shrinkage stress when the temperature increases. Due to the structure dispersion of polymeric materials, heating to a certain temperature can only diminish the internal stress to a certain extent. Intermolecular links of high energy barriers, including unstable crystallites, intermolecular forces, and entanglements need higher temperatures to diminish and relax. It is difficult to find, at this

Table VIIIB Unit-Cell Parameters of Ultra-Drawn PE (40) (Orthorhombic)

Draw Ratio	<i>a</i> (Å)	<i>b</i> (Å)	<i>c</i> (Å)	<i>d_c</i> (g/cm ³)
10	7.40	4.92	2.54	1.005
20	7.40	4.91	2.55	1.005
30	7.39	4.90	2.55	1.005
40	7.34	4.89	2.54	1.020
50	7.33	4.87	2.54	1.025
Bunn's data ¹⁹	7.40	4.93	2.534	1.008

Table IX Unit-Cell Parameters and Internal Stress of PP

Annealing Condition	<i>a</i> (Å)	<i>b</i> (Å)	<i>c</i> (Å)	(°)	<i>V</i> (Å ³)	Internal Stress (MPa)
Unset	7.12	6.51	21.96	99.8	1003	7.45
80°C						
15 min	7.05	6.49	21.82	99.4	985	8.23
100°C						
15 min	6.95	6.46	21.71	102.7	951	7.25
120°C						
15 min	6.89	6.44	21.43	100.1	935	7.06
140°C						
15 min	6.89	6.43	21.35	99.1	934	4.31
Published data ³⁸	6.630	6.504	20.78	99.5	909	—

Table X Unit-Cell Parameters of PPTA Fibers (Monoclinic)

Annealing Condition	<i>a</i> (Å)	<i>b</i> (Å)	<i>c</i> (Å)	(°)	<i>V</i> (Å ³)	Authors
Unset	7.19	5.18	12.9	90	480	Northolt (1974) ⁴²
500°C	7.87	5.18	12.9	90	521	Northolt (1974) ⁴²
	7.80	5.19	12.9	90	523	Tadokoro (1973) ⁴³
600°C	9.39	5.20	13.0	56.4	529	Yabuki (1975) ⁴⁴
Kevlar 49	7.78	5.28	12.9	90	530	Penn (1979) ⁴⁵

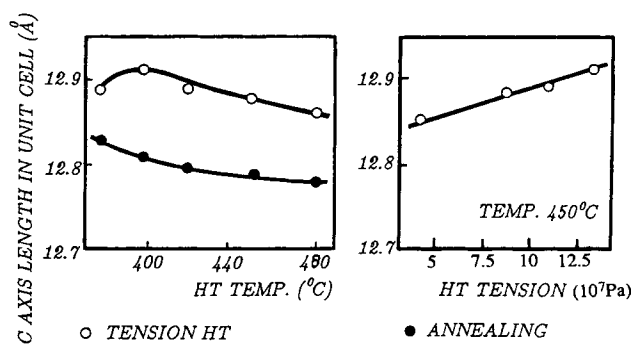
moment, an ideal structural model to evaluate the relation among internal stresses, crystalline deformations, moduli of crystals, oriented amorphous, and isotropic amorphous regions. Similar to the study of the influence of external stress on crystalline lattices, a simple series model has been adopted and it is supposed that there is the same internal stress transferring through crystalline and noncrystalline areas.

The release of thermal shrinkage stress by heating is accompanied by relaxation. In order to diminish the influence of the relaxation, the thermal shrinkage stress is measured with faster heating rate (20°C/min, method A) and the highest shrinkage stress for the sample at constant length could indicate the internal stress (Fig. 2). Otherwise, under a low temperature ascent, the polymer relaxation would lead to a decrease in the measured value of the thermal shrinkage stress. From Figures 3 and 4, it is seen that for PET after annealing the highest thermal shrinkage stress, i.e., the internal stress, decreases and the lattice deformation, orientation, and lattice modulus decrease as well.

There are two kinds of data showing in Figure 5, which express the relationship between the internal

stress and the tensile modulus of various polymers. Those of PET, PPTA, PE, PP, and PAN were obtained from our own experiments, and the data of PE-L was from previous studies.^{12,47} Two sets of data from PET and PPTA indicate that the higher the internal stress, the higher the tensile modulus. Each of them was from samples made of the same raw materials and with the same processing but different annealing conditions.

However, there are a lot of factors which influence the internal stress in polymers:

**Figure 1** C-Axis length of HT PPTA unit cell.

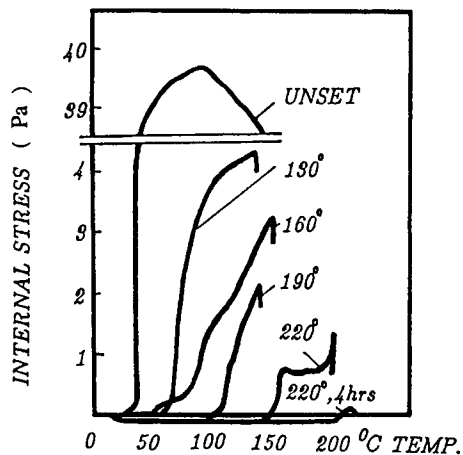


Figure 2 Shrinkage internal stress.

1. Amounts and relative locations of the crystalline and amorphous regions. During heating, in amorphous regions, the internal stress would come primarily from entropic shrinkage forces associated with the numbers of oriented molecules and/or the orientation distribution; polymer crystals would expand, which reduces the apparent thermal shrinkage and shrinkage force, i.e., the internal stress. In addition, for semicrystalline polymers, crystalline regions act as net point in the whole structure. These net points confine the release of the internal stress which appears only on the melting of corresponding crystallites at a certain temperature. On the other hand, some crystallites under the po-

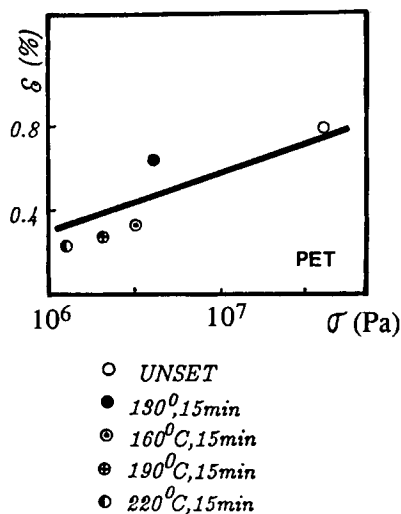


Figure 3 Shrinkage stress and lattice deformation.

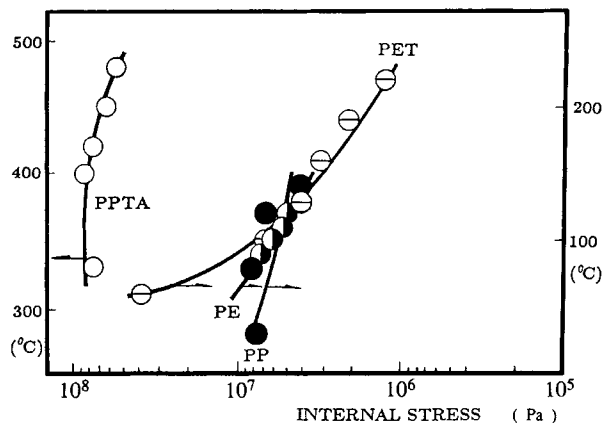


Figure 4 Annealing temp. vs internal stress.

tential internal stress would melt to be amorphous or recrystallize to affect the internal stress.

2. interactions between neighboring molecules,
3. the rigidity and flexibility of macromolecular chains,
4. molecular weights and their distributions,
5. molecular orientations and their distributions, and
6. different measurement procedures of the internal stress (especially the influence of molecule relaxations during examinations).

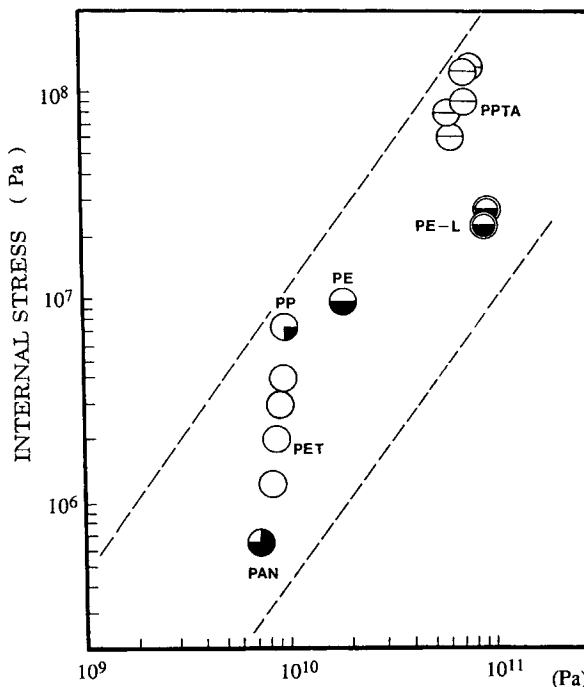


Figure 5 Internal stress vs modulus.

Therefore, it is difficult to obtain a simple linear relationship between the internal stress and the corresponding modulus for polymers. Nevertheless, when we put all these data (from various polymers including semicrystalline PET and PP, semirigid chain rod-like PPTA, flexible chain PE, and paracrystalline PAN) on one diagram, it is clearly seen that they are located in a zone which roughly reflects a linear relationship between the internal stress and the tensile modulus of oriented polymers (Fig. 5).

It is known that there are several ways to increase the internal stress which effectively improves the tensile modulus of polymeric materials:

1. Increase the orientation of macromolecules, which directly relates to the entropy change, a primary effect on the internal stress.
2. Increase the crystallinity. Crystallites existing in polymers serve the function of net points which confine relaxations of amorphous molecules and restrict the release of the internal stress. Then, the internal stress which alternatively goes through the amorphous and crystalline regions would be gradually released during the melting of crystallites.
3. Increase the molecular weight. Higher molecular weight would result in higher entropy difference between coil chain and extended chains and lead to more entanglements which also act as net points to hold the internal stress.
4. Increase the intermolecular forces.

Generally speaking, a series of technological procedures which could make the aforementioned requirements come true would benefit the tensile

modulus of polymers. For example, the drawing increases orientations and results in the increase of modulus. Heat treatments under tension or constant length which usually improve crystallinity and orientation would increase the internal stress and modulus. However, the heat treatment without tension, namely annealing, usually reduces orientation, which decreases the internal stress and lowers modulus. Liquid crystal polymers can be spun into ultra-highly oriented and crystalline fibers with ultra-high internal stress and modulus. Ultra-high molecular weight polyethylene fibers obtained through gel-spinning and ultra-drawing have very high internal stress and high performance mechanical properties.

In spite of the existing relation between the internal stress and modulus being available for all these studied polymers consisting of extended chain crystalline PPTA, flexible chain crystalline PE, semicrystalline PET and PP, and paracrystalline PAN, the relation between orientation and modulus is quite different. Although the orientation-modulus relation looks like a linear curve for each fiber sample, the polymers with different chemical structures and corresponding different molecular networks would possess different slopes and intercepts—because of orientation being a structure parameter and not a mechanical property. With different molecule structure, the same orientation would lead to different mechanical behaviors.

THERMAL MODULUS OF CRYSTALLINE LATTICE

The fiber thermal shrinkage modulus is the quotient of the maximum shrinkage stress (i.e., internal stress) divided by the shrinkage rate at a corre-

Table XI The Thermal Shrinkage Modulus of PET Fibers

	Heat-Setting Condition				
	Unset	130° 15 min	160° 15 min	190° 15 min	220° 15 min
Filament thermal shrinkage (%)	0.344	0.300	0.300	0.227	0.145
Filament thermal shrinkage modulus ($\times 10^{-8}$ dyn/cm ²)	11.5	1.40	1.06	0.956	0.897
Filament thermal modulus ($\times 10^{-9}$ dyn/cm ²)	10.4	8.52	6.34	4.02	—
Crystal modulus ($\times 10^{-9}$ dyn/cm ²)	50.0	6.65	9.38	8.03	5.80
Crystal modulus		1.27 $\times 10^2$ GPa (at room temperature) ⁴⁸			
Modulus of heat-set filament		1.09 $\times 10$ GPa (at room temperature) ⁴⁸			
Modulus of unset isotropic filament		0.47 GPa near T_g ; 1.76 GPa (at room temperature)			

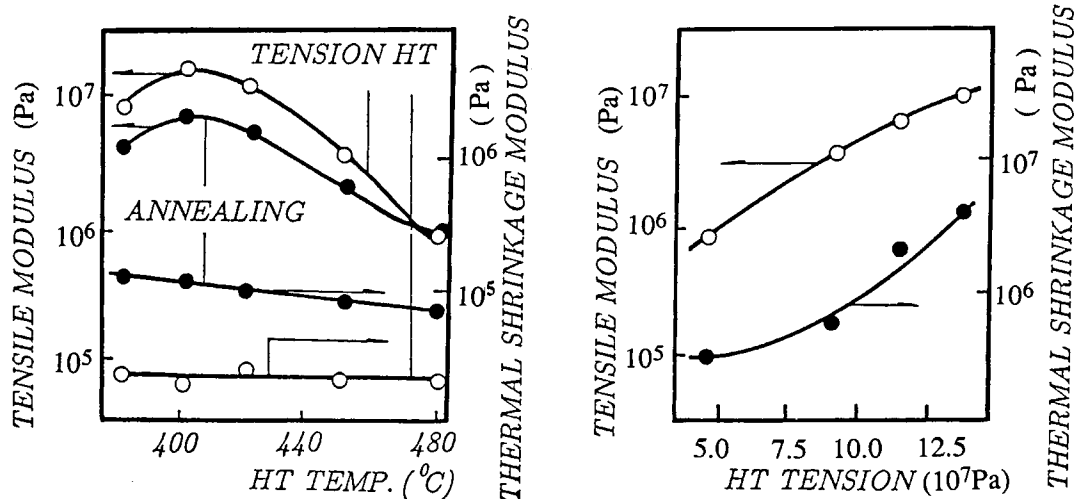


Figure 6 Tensile and thermal shrinkage modulus of PPTA crystalline region.

sponding temperature. Shrinkage stress is measured by the continuous temperature increase with constant fiber length. The thermal lattice (shrinkage) modulus is the quotient of the maximum shrinkage stress divided by the lattice deformation.

Table XI^{17,48} shows the thermal shrinkage moduli and the thermal lattice tensile moduli of PET fibers. Thermal tensile moduli measured at the corresponding temperature is one order higher than thermal shrinkage moduli. The thermal shrinkage modulus should then be equal to the thermal tensile modulus.

Figure 6 shows the thermal tensile moduli and the thermal shrinkage moduli of PPTA fibers at a series of temperatures. The thermal shrinkage modulus of PPTA slightly decreases with increasing annealing temperature, and the tensile modulus varies with the annealing temperature. At the same HT temperature, the thermal shrinkage modulus of PPTA varies with the tension of heat treatment. This means that thermal history, tension, and the lattice deformation can influence the shrinkage modulus. Therefore, the PE lattice moduli by different authors fluctuate considerably (Table XII⁴⁹) like that of PET. The deviations might be caused by the processing history and the internal stress.

CONCLUSION

Polymer processing, mainly drawing, causes orientation and internal stress which causes lattice deformation and raises tensile modulus of polymer. It is universal for crystalline polymers.

1. Compared to small molecule crystals, the unit cell parameters of polymer crystals are easy to vary to a certain extent. One of the reasons is that there are more defects in the polymer crystals. Lattice deformation of normal flexible chain PE crystal is rather small ($T_g < \text{room temperature}$), $< 2\%$. Lattice deformation of semirigid chain PPTA crystal is also small, $< 2\%$. The biggest deformation happens in PET crystals, whose chain rigidity is between those of PE and PPTA. The variation of the c -axis of PET is as high as about 10% . These differences might contribute to the crystal defects and crystal types. PE has flexible chains, which are easy to fold into

Table XII Theoretical and Measured Lattice Moduli⁴⁹ (GPa)

Theoretical Moduli	Measured Moduli	Methods	Authors
PE:			
182	235	WAXS	Treloar
340	150	WAXS	Zimautu et al.
290	255	WAXS	Mayasawa
256	358	Raman	Otasima et al.
315.5	290	Raman	Tashiro et al.
297	329	Neutron	Boudreaux
	270 (avg.)		
PP:			
49	34	WAXS	Ashina et al.
28			Miyasawa
33			Miyasawa

the crystal lattice. So, comparatively, its crystal contains less defects. PET has semi-flexible chains, which are not so easy to fold into the crystal lattices. Hence, in its crystal area, there are more defects. PPTA has rigid-rod molecules and forms extended chain crystals, which are different crystal types compared with both polymer crystals above. The higher the annealing temperature and the longer the HT time, the shorter the a , b , and c axes of the unit cell, the more integral and regular the lattice, and the smaller the unit cell volume. All these structural changes are related closely to the variations of the internal stress.

2. For glassy polymers, the internal stress is attributed to the entropy variations of molecule chains. For totally crystalline polymers, the deformations, defects, and orientations of crystallites contribute to the internal stress. For semicrystalline polymers, not only both of above contributions join together, but also affect each other. The crystalline regions

separate the amorphous regions and act as net points. During heating, these net points confine the relaxation of amorphous molecules and prohibit the release of the internal stress. But at the same time, the internal stress in amorphous regions promote the melting and recrystallization of these net point crystallites.

3. The internal stress frozen in materials is a characteristic of oriented polymers and fibers. The lattice deformation is, as well, one of the characteristics of conventional crystalline polymer fibers. Both internal stress and modulus of polymer materials are mechanical behaviors. There is a rough positive linear relationship between the internal stress and the modulus in our observed ranges despite the variation of polymers. It is apparent that the increase of the internal stress in polymer fibers would improve their tensile modulus. Technical processes which could increase internal stress would result in improving the mechanical properties of polymers.

APPENDIX

The Methods for Estimate Internal Stress in Polymers

There are two kinds of analyses to evaluate the internal stress in polymers, thermal mechanical analysis, and stress relaxation analysis.

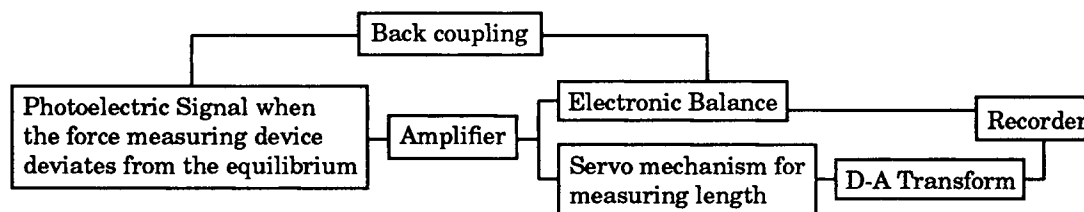
Thermal mechanical analysis adopts heat to release internal stress originally existing in oriented polymer materials. An oriented polymer sample (fiber or film) with two ends fixed in two clamps keeps constant length, then is heated to a certain temperature and the released shrinkage force is measured. It can still be divided into two methods: temperature dependent process (method A)

and time-dependent process (method B). Method C is based on the stress relaxation process.

Method A

Sample are continuously heated in a temperature range, and simultaneously measured as the corresponding shrinkage force appeared. Internal stress is indicated by the maximum shrinkage force in a certain temperature range.

In this paper, most of the internal stresses are estimated by method A, An XF-2 Multifunction Mechanical Analyzer⁵⁰ (self-made by China Textile University) was used. A block diagram of this instrument is given as follows:



It has some special features:

1. With this instrument, force is measured by means of a recording electronic balance, the reading of which is precise to a few milligrams when the total force is 40 g.
2. Length is automatically measured by means of a precision screw which is driven by servo-step motor, making possible the automatic measuring and recording of length changes. The screw can also be

positively driven to impart stretching to the sample at a rate from 0% up to a moderately high speed of 1000%/min when a test length of 20 mm is used.

3. The sample between the clamps can be surrounded either by air, inert atmosphere, or solvents, and can be raised or lowered suddenly in a period of 1–2 s.

During the thermal shrinkage force measurements, the samples, 20-mm length between two clamps, were surrounded by N₂ atmosphere. The data is recorded with temperature rising from room temperature to certain temperature, i.e., the so-called temperature-dependent process. The heating rate is 20°C/min.

In this paper, the internal stress data of PE-L were determined by means of a specially designed apparatus¹² (see Fig. 7). The sample with an approximately 80-mm length was plunged into a silicone oil bath and the transducer output recorded the shrinkage forces vs. temperature and heated at 10°C/min. The internal stress is also indicated by maximum shrinkage force.

Method B

One of the apparatuses which could be applied for time-dependent shrinkage force measurement is the type shown in Figure 7. The sample can be suddenly moved into a silicone oil bath with constant elevated temperature. The transducer output records the shrinkage forces as a function of time. Also, the internal stress is indicated by the maximum shrinkage force.

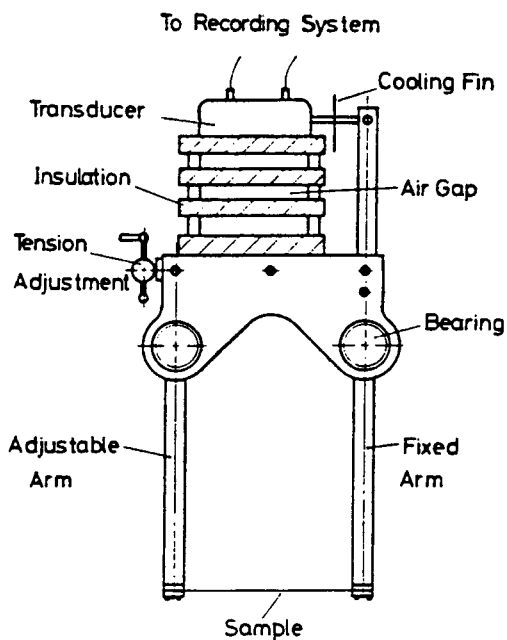


Figure 7 Schematic diagram of the apparatus used for the measurements of shrinkage force in isothermal experiments.

Method C

The method used to determine the internal stress (σ_i) level was based on an analysis of the kinetics of stress relaxation in the sample under study.⁵¹ The method, originally used for metals, has been applied by the authors to polyethylene; it utilizes the applicability of the power law for stress relaxation at sufficiently long periods of time. The power law can be written as

$$\sigma - \sigma_i = K(t + \alpha)^{-n} \quad (\text{A1})$$

where σ and σ_i denote the stress and the internal stress, respectively, t the time and α , n , and K constants. Plotting $(-d\sigma/d \log t)$ vs. σ , a straight line is obtained, having a slope of $2.3 n$, and intercepting the σ -axis at σ_i .

This project is supported by the National Science Foundation of China.

REFERENCES

1. J. W. Tobias and L. J. Taylor, *J. Appl. Polym. Sci.*, **19**, 1317 (1975).
2. R. G. C. Arridge, P. J. Barham, and A. Keller, *J. Polym. Sci.*, **15**, 389 (1977).
3. A. Ram, Z. Tadmor, and M. Schwartz, *Int. J. Polym. Mater.*, **6**, 55 (1977).
4. F. Decandia, R. Russo, V. Vittoria, and A. Peterlin, *J. Polym. Sci. Polym. Phys. Ed.*, **20**, 1175 (1982).
5. R. D. Andrews, *J. Appl. Phys.*, **26**, 1061 (1955).
6. S. W. Allison, P. R. Pinnock, and I. M. Ward, *Polymer*, **7**, 66 (1966).
7. Y. Tanabe and H. Kanetsuna, *Polymer*, **20**, 1121 (1979).
8. M. Trznadel and M. Kryszewski, *Polymer*, **29**, 418 (1988).
9. M. Trznadel, *Polymer*, **27**, 871 (1986).
10. T. Pakula and M. Trznadel, *Polymer*, **26**, 1011 (1985).
11. P. R. Pinnock and I. M. Ward, *Trans. Faraday Soc.*, **62**, 1308 (1966).
12. N. Kahar, A. R. Duckett, and I. M. Ward, *Polymer*, **19**, 136 (1978).
13. F. Pietsch, R. A. Duckett, and I. M. Ward, *Polymer*, **20**, 1133 (1979).
14. G. Capaccio and I. M. Ward, *Colloid Polym. Sci.*, **260**, 46 (1982).
15. H. Wang, PhD Thesis at China Textile Univ. (1988).
16. I. Sakurada and K. Kaji, *J. Polym. Sci. Part C*, **31**, 57 (1970); C. Sawatari and M. Matsuo, *Macromolecules*, **19**, 2653 (1986).
17. A. Zhang, H. Jiang, C. Wu, L. Zhou, L. Xuan, and B. Qian, *Textile Res. J.*, **7**, 387 (1985).
18. W. T. Astbury and C. J. Brown, *Nature*, **158**, 871 (1946).
19. R. de P. Daubeny, C. W. Bunn, and C. J. Brown, *Proc. Roy. Soc. (London)*, **A226**, 531 (1954).

20. H. G. Kilian, H. Halboth, and E. Jenkel, *Kolloid-Z. Polymer*, **172**, 166 (1960).
21. Yu Ya Tomashpol'skii and A. S. Markova, *Vysokomolekul Soedin.*, **6**, 27 (1964); *Polym. Sci.*, (USSR) (English tran.) **6**, 316 (1964).
22. S. Fakirov, E. W. Fischer, and G. F. Schmidt, *Macromol. Chem.*, **176**, 2459 (1975).
23. Y. Kinoshita, R. Nakamura, Y. Kitano, and T. Ashida, *Polymer Preprint*, **20**(1), 454 (1979).
24. H. Zahn and R. Krizikalla, *Macromol. Chem.*, **23**, 3 (1957).
25. S-B Lin and J. L. Koenig, *J. Polym. Phys. Ed.*, **20**(12), 2277 (1982).
26. T. Thistlethwaite, R. Jakeways, and I. M. Ward, *Polymer*, **29**(1), 61 (1988).
27. T. Sun, A. Zhang, F. Li, and R. S. Porter, *Polymer*, **29**(12), 2115 (1989).
28. C. W. Bunn, *Trans. Faraday Soc.*, **35**, 482 (1939).
29. E. R. Wolter and F. P. Reding, *J. Polym. Sci.*, **21**, 561 (1956).
30. P. R. Swan, *J. Polym. Sci.*, **42**, 525 (1960); P. R. Swan, *J. Polym. Sci.*, **56**, 403 (1962).
31. H. Kojima and K. Yamaguchi, *Kobunshi Kagaku*, **19**, 715 (1962).
32. P. Zugenmaier and H-J Cantow, *Kolloid-Z. Polym.*, **230**, 229 (1969).
33. A. Chiba, H. Futama, and J. E. Furuichi, *Reports. Progr. Polym. Phys. Japan*, **7**, 51 (1964).
34. G. Natta and P. Conadini, *Nuovo Cimento.*, 15 (Suppl.), 40 (1960).
35. Z. Mfncik, *Chem. Prumysl*, **10**, 377 (1960).
36. A. Turner-Jones, J. M. Aizlewood, and P. R. Beckett, *Macromol. Chem.*, **75**, 134 (1964).
37. M. Hikosaka and T. Seto, *Reports. Progr. Polym. Phys. Japan*, **12**, 153 (1969).
38. Z. W. Wilchinsky, *J. Appl. Phys.*, **31**, 1969 (1960).
39. Z. Hu, A. Zhang, H. Jiang, and C. Wu, *J. of China Textile Univ.* (English Ed.), No. 1 (1987).
40. A. Zhang, K. Chen, P. Lu, Z. Hu, and Z. Wu, *Bull. Am. Phys. Soc.*, **33**(3), 504 (1988).
41. H. Jiang, C. Wu, A. Zhang, and P. Yang, *Compos. Sci. Technol.*, **29**, 33 (1987).
42. M. G. Northolt, *Eur. Polym. J.*, **10**, 799 (1974).
43. K. Tashiro, M. Kobayashi, and H. Tadokoro, *Macromolecules*, **10**, 413 (1977).
44. Kazuyuki Yabuki, Hiroshi Ito, and Toshiko Ota, *Sen-i Gakkaishi*, **31**, T-524 (1975); **32**, T-55 (1976).
45. N. Penn, *J. Appl. Polym. Sci.*, **23**(1), 59 (1979).
46. Z. Wu, J. Zhou, Q. Wu, A. Zhang, B. Huang, and B. Qian, *J. Textile Res.* (Chinese), **7**(5), 261 (1986).
47. W. J. Lyon, *J. Appl. Phys.*, **29**, 1429 (1958).
48. Taisuke Ito, *Sen-i Gakkaishi*, **38**(1), P-54 (1982).
49. G. Capacco, J. Clements, P. J. Hine, and I. M. Ward, *J. Polym. Phys. Ed.*, **19**, 1435 (1981).
50. Baojun Qian, T. Hongjiang, Y. Pingyu, and Z. Wu, *J. of Engineering for Industry*, **105**, 88 (1983).
51. J. Kubt, J. Petermann, and M. Rigdahl. *J. Mater. Sci.*, **10**, 2075 (1975).

Received July 12, 1989

Accepted June 22, 1990